

Boletus aereus protects against acute alcohol-induced liver damage in the C57BL/6 mouse via regulating the oxidative stress-mediated NF- κ B pathway

Luping Zhang^{a*}, Bo Meng^{a,b*}, Lanzhou Li^{b*}, Yanzhen Wang^{b,c}, Yuanzhu Zhang^b, Xuexun Fang^{a,b} and Di Wang^{b,c}

^aGastroenterology and Endoscopy Center, The First Bethune Hospital of Jilin University, Jilin University, Changchun, China; ^bKey Laboratory for Molecular Enzymology and Engineering of Ministry of Education, School of Life Sciences, Jilin University, Changchun, China; ^cSchool of Pharmacy Food Science, Zhuhai College of Jilin University, Zhuhai, China

ABSTRACT

Context: Alcoholic liver disease, caused by abuse and consumption of alcohol, exhibits high morbidity and mortality. *Boletus aereus* Bull. (Boletaceae) (BA) shows antioxidant, anti-inflammatory and antimicrobial effects.

Objectives: To investigate the hepatoprotective effects of BA using an acute alcohol-induced hepatotoxicity mice model.

Materials and methods: The composition of BA fruit body was first systematically analyzed. Subsequently, a C57BL/6 mice model of acute alcohol-induced liver injury was established by intragastrically administration of alcohol, which was intragastrically received with BA powder at 200 mg/kg and 800 mg/kg for 2 weeks, 60 mg/kg silybin treatment was used as positive control group. By employing the pathological examination, ELISA, RT-PCR and western blot, the regulation of BA on oxidative stress signals was investigated.

Results: The LD₅₀ of BA was much higher than 4 g/kg/p.o. In acute alcohol-damaged mice, BA reduced the levels of alanine aminotransferase (>18.3%) and aspartate aminotransferase (>27.6%) in liver, increased the activity of liver alcohol dehydrogenase (>35.0%) and serum acetaldehyde dehydrogenase (>18.9%). BA increased the activity of superoxide dismutase (>13.4%), glutathione peroxidase (>11.0%) and 800 mg/kg BA strongly reduced chemokine (C-X-C motif) ligand 13 (14.9%) and chitinase-3 like-1 protein (13.4%) in serum. BA reversed mRNA over-expression (>70%) and phosphor-stimulated expression (>45.0%) of an inhibitor of nuclear factor κ -B kinase (NF- κ B, an inhibitor of nuclear factor κ -B α and nuclear factor κ -B in the liver.

Conclusions: BA is effective in ameliorating alcohol-induced liver injury through regulating oxidative stress-mediated NF- κ B signalling, which provides a scientific basis for further research on its clinical applications.

ARTICLE HISTORY

Received 3 March 2020
Revised 9 August 2020
Accepted 15 August 2020

KEYWORDS





Hepatoprotective; alcohol metabolism; inflammation; reactive oxygen species

Introduction


Alcoholic liver disease (ALD), caused by the abuse and consumption of alcohol, exhibits extremely high morbidity and mortality (Ren et al. 2018). Continued heavy alcohol consumption will exacerbate alcoholic fatty liver disease (AFLD), which develops into fatty hepatitis, liver fibrosis and even hepatic carcinoma (Gao and Bataller 2011). About 90% of alcohol is metabolized in the liver to acetaldehyde by alcohol dehydrogenase (ADH), and then decomposes into acetic acid under the metabolism of acetaldehyde dehydrogenase (ALDH), before finally being converted into non-toxic and harmless substances (Jelski et al. 2008). However, heavy alcohol consumption damages the liver cells, resulting in a decrease in the activity of the above enzymes, thus causing the accumulation of acetaldehyde, which is responsible for alcoholism (Setshedi et al. 2010).

Among the cellular components most vulnerable to acetaldehyde are the mitochondria, where in mitochondrial damage

induces the over-accumulation of reactive oxygen species (ROS) and the suppression of antioxidant activities (Farfan Labonne et al. 2009). Under physiological conditions, ROS are efficiently eliminated by antioxidant defense systems including superoxide dismutase (SOD) and glutathione peroxidase (GSH-Px) (Dai et al. 2016). However, hyper-levels of ROS, acting as a secondary messenger, enhance the signal transduction of nuclear factor kappa B (NF- κ B), a reduction/oxidation (redox)-sensitive factor, from the cytoplasm into the nucleus (Bubici et al. 2006). Normally, NF- κ B binds to the inhibitor of nuclear factor kappa-B (I κ B) protein to form a complex that blocks the nuclear localization signal of NF- κ B. However, when the cells are stimulated by alcohol, I κ B protein is phosphorylated by the activated I κ B kinase and then the nuclear localization signal of NF- κ B is exposed and NF- κ B is transported into the nucleus (Wu et al. 2014). The inhibition of NF- κ B activation and cytokine synthesis is a potential mechanism for the treatment of alcohol-induced liver injury (Abhilash et al. 2014).

CONTACT Xuexun Fang  fangxx@jlu.edu.cn  School of Life Sciences, Jilin University, Qianjin Street 2699, Changchun 130012, China; Di Wang  jluwangdi@jlu.edu.cn  School of Life Sciences, Jilin University, Qianjin Street 2699, Changchun 130012, China

*These authors contributed equally to this work.

 Supplemental data for this article can be accessed [here](#).

© 2020 The Author(s). Published by Informa UK Limited, trading as Taylor & Francis Group.

This is an Open Access article distributed under the terms of the Creative Commons Attribution-NonCommercial License (<http://creativecommons.org/licenses/by-nc/4.0/>), which permits unrestricted non-commercial use, distribution, and reproduction in any medium, provided the original work is properly cited.

Presently, raw materials for liver cell metabolism, agents for alcohol metabolism and opioid receptor antagonists are among the commonly used ALD treatment clinically (Ozkol et al. 2017). However, after chronic administration of these agents, various adverse effects including drug dependence, vomiting, dermatitis, dizziness and leukopenia are noted in ALD patients (Triantafyllou et al. 2010). Natural products, especially fungi, show considerable biological effects in humans.

In our group, *Antrodia camphorata* (Fomitopsidaceae) has been confirmed to display hepatoprotective effects in acute alcohol-induced mice via regulating oxidative stress signalling (Liu et al. 2017). *Boletus aereus* Bull. (Boletaceae) (BA), rich in carbohydrates, amino acids and fatty acids and widespread in Europe (Beugelsdijk et al. 2008), shows a variety of biological functions such as antioxidant (Zheng et al. 2014), anti-inflammatory (Wu et al. 2016), antitumor (Lemieszek et al. 2017) and antimicrobial (Kosani et al. 2017) properties. BA polysaccharides can increase the activities of antioxidant enzymes and reduce the lipid peroxidation in mice administered with alcohol (Guo et al. 2015). However, the effects of BA on acute alcohol-induced liver injury and its underlying mechanisms have not been systematically reported.

In this study, we first systematically analysed the components of BA fruiting bodies. Subsequently, BA's hepatoprotective effects and the underlying mechanisms related to oxidative stress-mediated NF- κ B signalling, were explored systematically in mouse models with acute alcohol-induced hepatotoxicity. Our data provide valuable evidence to support the use of BA as a functional food to treat ALD.

Materials and methods

B. aereus compounds analysis

B. aereus fruiting bodies, purchased from TengHui Agriculture (Kunming, Yunnan, China), were verified by professor Li Yu from Jilin Agricultural University and dried at $60 \pm 2^\circ\text{C}$, crushed and passed through a 60-mesh sieve.

Main components detection

The quantities of the main components including total sugar, reducing sugar, total protein, total ash, crude fat, total flavonoids, total triterpenes, mannitol, nucleotides, vitamins, sterols and polyphenols were measured using the phenol-sulfuric acid method (Jain et al. 2017), 5-dinitrosalicylic acid colorimetric estimation (Zhang et al. 2014), Kjeldahl method (Chromy et al. 2015), ash content analysis, Soxhlet extraction (Smith and Tschinkel 2009), aluminium chloride colorimetry (Manurung et al. 2017), vanillin-glacial acetic acid-perchloric acid colorimetry (Li et al. 2014), iodometry (Rivera-Jacinto et al. 2009), high performance liquid chromatography (HPLC) (Mattila et al. 2001; Krpan et al. 2009), UV spectrophotometric assay (Araújo et al. 2013) and Folin-Ciocalteu method (Musci and Yao 2017), respectively.

Amino acids detection

The appropriate amounts of BA samples dissolved in 6 mol/L hydrochloric acid were hydrolyzed at $110 \pm 1^\circ\text{C}$ for 22 h, then dried under vacuum. Buffer (1 mL, 19.6 g sodium citrate and 16.5 mL hydrochloric dissolved in 1 L of deionized water, pH 2.2) was added to prepare test samples. The amino acids content

was quantified by an automatic amino acid analyzer (L-8900, Hitachi, Tokyo, Japan).

Mineral content detection

The levels of mercury (Hg), lead (Pb), selenium (Se), arsenic (As), cadmium (Cd), zinc (Zn), iron (Fe), manganese (Mn), chromium (Cr), calcium (Ca), copper (Cu), sodium (Na) and potassium (K) were detected by inductively coupled plasma optical emission spectrometry (Hurel et al. 2017).

Fatty acid detection

BA powder was extracted with a solution mixture of ether: petroleum ether (1:1) for 24 h. The crude fatty acid was dehydrated with anhydrous sodium sulphate and then methyl-esterified with 5% potassium hydroxide-methanol solution and the fatty acid content determined by gas chromatography-mass spectrometry (QP2010, Shimadzu, Tokyo, Japan).

Animal experiments

Healthy male C57BL/6 mice (8–10 weeks; 18–22 g) (SCXK (LIAO) 2015-0001) were obtained from Liaoning Changsheng Biotechnology Co., Ltd. (Liaoning, China). The mice were kept in a controlled environment at a temperature of $23^\circ\text{C} \pm 1^\circ\text{C}$ with $50\% \pm 10\%$ humidity and a 12-h light-dark cycle and free access to water and food.

Acute oral toxicity study

The experimental protocol was carried out under the Ethical Committee of Animal Research of Jilin University (2017SY010). The male C57BL/6 mice ($n=8$) were intragastrically administered with 4 g/kg of BA (the maximum intragastric dose), and then observed continuously for the first 4 h for any mortality changes and abnormal behaviours, intermittently for the next 24 h, and occasionally thereafter for 14 days for any delayed effects.

Animal model development and drug treatment process

The animal experiment was carried out in accordance with the Guiding Principles of Jilin University Animal Ethics Committee (2017SY0106). As a clinically used liver protectant, silybin (Sil) can reduce oxidative stress, and prevent the increase of alanine aminotransferase (ALT), tumour necrosis factor- α (TNF- α) and lipid peroxidation. Based on its clinically used doses, 60 mg/kg of Sil was chosen for the present experiments. The mice were fed for 7 days to acclimatize to the environment, and then randomly divided into five groups ($n=10$). The control mice were intragastrically administered with saline at 0.1 mL/10 g twice per day at 9:00 am and 4:00 pm for 14 days. All other mice were intragastrically administered with 13 g/kg of 56% ethanol (Erguotou wine, Beijing Shunxin Agricultural Co. Ltd, China) at 9:00 am once a day. After 7 h, the mice were intragastrically administered with saline at 0.1 mL/10 g body weight (model group; $n=10$), 60 mg/kg of Sil (Tianjin Tasly Sants Pharmaceutical Co. Ltd, China) (positive control group; $n=10$) and BA at doses of 200 mg/kg and 800 mg/kg (BA-treated groups; $n=10$) at 4:00 pm (Supplementary Figure 1S). The administration lasted for 14 days,

and the body weight of each mouse was monitored daily. After the last treatment, the mice were fasted overnight, and then blood was sampled from the caudal vein of each mouse. After the mice were sacrificed under euthanasia, organs including liver and kidney were quickly collected, and portions of the organs were fixed in 10% formalin buffer, while the remaining parts were stored at -80°C . The organ index was calculated by the following formula:

$$\text{Organ index}(\text{mg}/10\text{g}) = \text{organ weight}(\text{mg})/\text{body weight}(10\text{g})$$

Biochemical indicators detection

A portion of the liver tissues were homogenized with physiological saline on ice and centrifuged at 3500 rpm for 10 min.

The levels of aspartate aminotransferase (AST; CK-E90386M), ALT (CK-E90314M), ADH (CK-E92648M), ALDH (CK-E92649M), chemokine (C-X-C motif) ligand 13 (CXCL13; CK-E95658M), chitinase-3 like-1 protein (YKL-40; CK-E95772M), thrombopoietin (TPO; CK-E93965M), interleukin-7 (IL-7; CK-E20125M), plasminogen activator inhibitor type 1 (PAI-1; CK-E93562M), retinol-binding protein 4 (RBP4; CK-E20170M), nitric oxide (NO; CK-E20293M), ROS (CK-E91516M), SOD (CK-E20348M), catalase (CAT; CK-E92636M), GSH-Px (CK-E92669M) and malondialdehyde (MDA; CK-E20347M) in the serum and liver and the levels of high-density lipoprotein (HDL; CK-E91912M) and total cholesterol (TC; CK-E91839M) in the liver were detected using enzyme-linked immunosorbent assay (ELISA) kits purchased from Shanghai Yuanye Biological Technology Co., Ltd. (Shanghai, China) according to the instruction manuals.

Histopathological examination

Portions of the liver and kidneys were excised and fixed in 10% neutral formalin buffer. Afterwards, the fixed tissues were dehydrated with gradient ethanol (70, 80, 90, 95 and 100%), and then samples were cleared twice in xylene, and embedded in paraffin. The paraffin samples were sliced into $5\ \mu\text{m}$ thickness, and then stained with haematoxylin and eosin (H&E). After dehydration, the pathological sections were observed under a light microscope ($400\times$) (Olympus, Tokyo, Japan) and photographed.

Reverse transcription-polymerase chain reaction (RT-PCR)

RT-PCR was performed according to a method described previously with some modification (Zhang et al. 2017). Briefly, the RNA was isolated from the liver of mice using Trizol (Invitrogen, USA), and then synthesized by QuantScript RT Kit (Tiangen Biotech (Beijing) Co. Ltd., China). β -Actin primers were used as an internal control. The conditions of PCR amplification were as follows: denaturation at 95°C for 5 min, followed by 36 cycles at 95°C for 45 s, 57°C for 45 s and 72°C for 45 s. The primer sequences are listed in Supplementary Table 1S.

Western blot analysis

A portion of the liver tissues was homogenized with radio-immunoprecipitation assay (RIPA, Sigma-Aldrich) lysate containing 2% phenylmethanesulfonyl fluoride (PMSF, Sigma-Aldrich, St. Louis, MO) and 1% protease inhibitor cocktail (Sigma-

Aldrich, St. Louis, MO). The total protein concentration was determined using the BCA protein assay kit (Merck Millipore, Burlington, MA). Proteins ($40\ \mu\text{g}$) were boiled at 100°C for 5 min with loading buffer (Solarbio Biotechnology Co., Ltd, Beijing, China), separated by 12% polyacrylamide gel and transferred onto $0.45\ \mu\text{m}$ polyvinylidene fluoride (PVDF) membranes (Merck Millipore, Burlington, MA). The membranes were blocked using 5% bovine serum albumin (BSA) (Sigma-Aldrich, St. Louis, MO) and solubilized with Tris-buffered saline (TBS) at 4°C for 4 h. The blocked membranes were incubated with primary antibody against phosphor (P)-inhibitor of nuclear factor kappa-B kinase α/β (IKK α/β) (ab195907), total (T)-IKK α/β (ab178870), P-IkB α (ab12135), T-IkB α (ab32518), P-NF- κ B p65 (ab86299), T-NF- κ B p65 (ab7970) (Abcam, Cambridge Science Park, UK) and glyceraldehyde-3-phosphate dehydrogenase (GAPDH) (ABS16; Merck Millipore, Burlington, MA) at 4°C overnight. The membranes were washed five times with TBS containing Tween 20, and then incubated in horseradish peroxidase-conjugated goat anti-rabbit (IH-0011; Dingguo, Beijing, China) and goat anti-mouse secondary antibody (IH-0031; Dingguo, Beijing, China) diluted 2000-fold with 2% BSA for 4 h at 4°C . The blots were visualized using Immobilon Western Chemiluminescent HRP Substrate (WBKLS0500; Merck Millipore, Burlington, MA) and Gel Imaging System (Tanon Technology Co., Ltd., Shanghai, China). Quantitative gray-scale analysis of each protein band was performed using Image J analysis software.

Statistical analysis

All statistical analyses were performed using SPSS 23.0 software (IBM Corporation, USA) and the data were presented as mean \pm standard errors of the mean (S.E.M.). Differences were tested by one-way analysis of variance (ANOVA). p values of < 0.05 were considered statistically significant.

Results

Composition of BA

For the main components of BA, 30.60% was total sugar, 4.80% was reducing sugar, 1.44% was triterpenes, 0.23% was flavonoids, 17.90% was mannitol, 12.20% was crude fat, 24.30% was total protein, 2.03% was polyphenols, 1.40% was sterols, 0.02% was vitamin B₂ and 0.42% was vitamin B₃; however, adenosine and vitamin A, B₁, B₆, C, D₂, D₃ and E were not detected (Table 1). A total of 17 amino acids were determined, among which the contents of methionine (0.60%), glutamic acid (0.39%) and aspartic acid (0.32%) were higher than those of the others (Table 1). Among the 13 detected minerals, K, Fe and Na were the most abundant (Table 1). Thirty-five fatty acids were measured, among which the contents of linoleic acid, oleic acid and hexadecanoic acid were significantly higher than those of the other fatty acids; however, capric acid, undecanoic acid, tridecanoic acid, myristoleic acid, *cis*-10-pentadecenoic acid, elaidic acid, *trans*-linoleic acid, α -linolenic acid, γ -linolenic acid, dihomogamma-linolenic acid, eicosapentaenoic acid, *cis*-13,16-docosadienoic acid methyl ester, docosahexaenoic acid and octanoic acid were not detected (Table 1).

Table 1. Composition of BA.

	Compounds	Contents	Compounds	Contents	
Main components (%)	Total sugar	30.60	Mannitol	17.90	
	Total ash	5.60	Protein	24.30	
	Total triterpenes	1.44	Total flavonoids	0.23	
	Reducing sugar	4.80	Nucleotide	ND	
	Crude fat	12.20	Sterols	1.40	
	Polyphenols	2.03	Vitamin A	ND	
	Vitamin B ₁	ND	Vitamin B ₂ ($\times 10^{-3}$)	1.71	
	Vitamin B ₃ ($\times 10^{-2}$)	4.16	Vitamin B ₆	ND	
	Vitamin C	ND	Vitamin D ₂	ND	
	Vitamin D ₃	ND	Vitamin E	ND	
	Amino acid (%)	Aspartic acid (Asp)	0.32	Isoleucine (Iso)	0.18
		L-Threonine (Thr)	0.21	Leucine (Leu)	0.30
		Serine (Ser)	0.19	Tyrosine (Tyr)	0.16
Glutamic acid (Glu)		0.39	Phenylalanine (Phe)	0.18	
Glycine (Gly)		0.30	Lysine (Lys)	0.16	
Alanine (Ala)		0.26	Histidine (His)	0.16	
Cystine (Cys)		0.03	Arginine (Arg)	0.17	
Valine (Val)		0.15	Proline (Pro)	0.15	
Methionine (Met)		0.60			
Minerals (%)		Mercury (Hg) ($\times 10^{-5}$)	8.76	Manganese (Mn) ($\times 10^{-3}$)	2.38
		Lead (Pb) ($\times 10^{-3}$)	2.32	Chromium (Cr) ($\times 10^{-4}$)	2.27
	Selenium (Se) ($\times 10^{-4}$)	6.81	Calcium (Ca) ($\times 10^{-2}$)	1.83	
	Arsenic (As) ($\times 10^{-5}$)	6.58	Copper (Cu) ($\times 10^{-3}$)	2.70	
	Cadmium (Cd) ($\times 10^{-5}$)	8.32	Sodium (Na) ($\times 10^{-2}$)	2.56	
	Zinc (Zn) ($\times 10^{-2}$)	1.02	Potassium (K)	1.74	
	Iron (Fe) ($\times 10^{-2}$)	3.78			
	Fatty acid (%)	Capric acid (C10:0)	ND	γ -Linolenic acid (C18:3n6)	ND
		Undecanoic acid (C11:0)	ND	Arachidic acid (C20:0) ($\times 10^{-3}$)	5.44
Lauric acid (C12:0) ($\times 10^{-4}$)		3.60	Paullinic acid (C20:1) ($\times 10^{-3}$)	7.34	
Tridecanoic acid (C13:0)		ND	Eicosadienoic acid (C20:2) ($\times 10^{-3}$)	3.62	
Myristic acid (C14:0) ($\times 10^{-3}$)		6.63	Eicosatrienoic acid (C20:3n3) ($\times 10^{-4}$)	9.78	
Myristoleic acid (C14:1n5)		ND	Dihomo-gamma-linolenic acid (C20:3n6)	ND	
Pentadecanoic acid (C15:0) ($\times 10^{-2}$)		1.73	Arachidonic acid (C20:4n6) ($\times 10^{-3}$)	2.71	
Cis-10-pentadecenoic acid(C15:1n5)		ND	Eicosapentaenoic acid (C20:5n3)	ND	
Hexadecanoic acid (C16:0)		0.96	Heneicosanoic acid (C21:0) ($\times 10^{-3}$)	1.58	
Palmitoleic acid (C16:1n7)		0.03	Docosanoic acid (C22:0) ($\times 10^{-2}$)	1.53	
Heptadecanoic acid (C17:0)		0.01	Erucic acid (C22:1n9) ($\times 10^{-3}$)	1.87	
Heptadecenoic acid (C17:1n7)		0.01	Cis-13,16-Docosadienoic acid Methyl ester (C22:2)	ND	
Stearic acid (C18:0)		0.18	Docosahexaenoic acid (C22:6n3)	ND	
Oleic acid (C18:1n9)		1.23	Tricosanoic acid (C23:0) ($\times 10^{-3}$)	1.72	
Elaidic acid (C18:1n9t)		ND	Tetracosanoic acid (C24:0) ($\times 10^{-2}$)	1.85	
Linoleic acid (C18:2n6c)		2.66	Nervonic acid (C24:1n9) ($\times 10^{-3}$)	6.74	
Translinoleic acid (C18:2n6t)		ND	Octanoic acid (C8:0)	ND	
α -Linolenic acid (C18:3n3)		ND			

ND: not detected.

Table 2. The effects of BA and Sil on the levels of ALT, AST, ADH and ALDH in serum and liver of alcohol-treated mice.

	CTRL	Alcohol (13 g/kg)			
		Model	Sil (60 mg/kg)	BA (200 mg/kg)	BA (800 mg/kg)
Serum					
AST (U/L)	127.8 \pm 1.6	147.8 \pm 2.6 [#]	134.2 \pm 2.7	137.9 \pm 3.0	133.4 \pm 6.5
ALT (U/L)	47.4 \pm 0.6	53.5 \pm 0.4 [#]	48.4 \pm 0.7	51.7 \pm 1.6	50.0 \pm 0.9
ALDH (μ mol/L)	8.6 \pm 0.2	7.4 \pm 0.2 [#]	8.6 \pm 0.1 [*]	10.0 \pm 0.3 ^{**}	8.8 \pm 0.3 [*]
Liver					
AST (U/g)	55.0 \pm 0.6	65.3 \pm 1.8 [#]	57.3 \pm 1.0 [*]	43.2 \pm 2.4 ^{**}	47.3 \pm 2.3 ^{**}
ALT (U/g)	17.1 \pm 0.3	20.2 \pm 0.5 [#]	18.2 \pm 0.4	16.5 \pm 1.1 [*]	14.0 \pm 0.7 ^{**}
ALDH (μ mol/g)	4.8 \pm 0.1	3.3 \pm 0.1 ^{##}	5.0 \pm 0.1 ^{**}	3.2 \pm 0.2	3.3 \pm 0.1
ADH (ng/mg)	2.6 \pm 0.1	2.0 \pm 0.2 ^{##}	2.8 \pm 0.1 ^{**}	2.7 \pm 0.2 ^{**}	3.2 \pm 0.2 ^{***}

All data are presented as mean \pm S.E.M. (n = 10).[#]p < 0.05, ^{##}p < 0.01 compared with control group; ^{*}p < 0.05, ^{**}p < 0.01 and ^{***}p < 0.001 compared with alcohol group.

Acute oral toxicity analysis

Compared to the control group, there was no obvious behaviour abnormality in 4 g/kg of BA-treated mice. In this study, due to the 4 g/kg of BA is the maximum intragastric dose, its LD₅₀ must be much higher than 4 g/kg.

Hepatoprotective effect of BA

Compared with normal mice, the bodyweight of alcohol-only treated mice lost 18.1% significantly at 7th day (p < 0.05; [Supplementary Table 2S](#)). During the 2-week treatment period, relative to the alcohol-only treated mice, BA and Sil failed to influence the bodyweight of the mice (p > 0.05; [Supplementary Table 2S](#)).

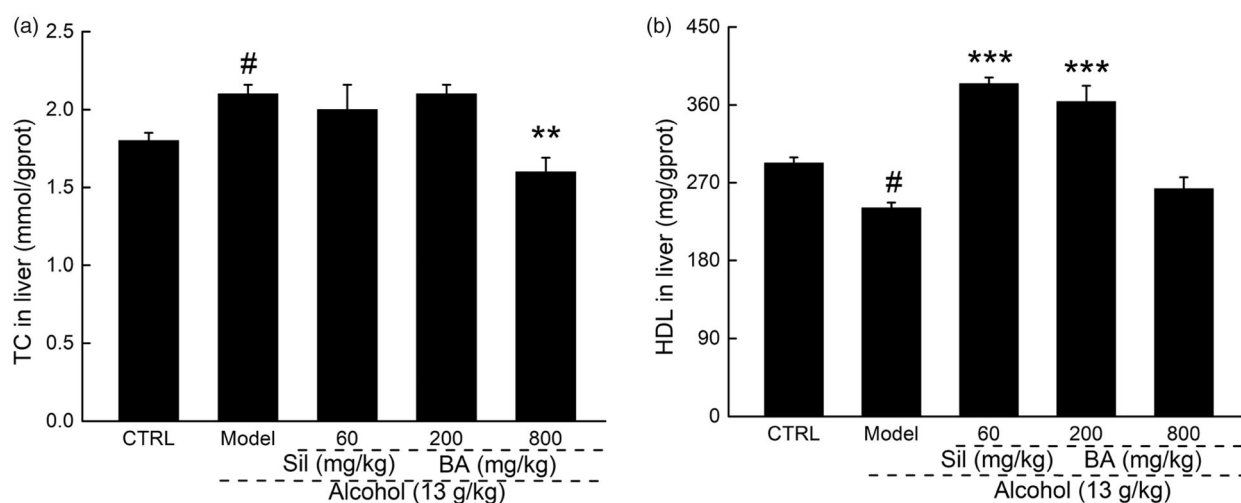


Figure 1. The effects of BA on hepatic levels of TC and HDL in mice with acute alcohol-induced liver injury. Two-week BA and Sil treatment (a) reduced the levels of TC and (b) increased the levels of HDL in the liver of mice with acute alcohol-induced liver injury. The data were analysed using a one-way ANOVA and expressed as means \pm S.E.M. ($n = 10$). # $p < 0.05$ vs. non-alcohol control group; ** $p < 0.01$ and *** $p < 0.001$ vs. alcohol-treated model group. BA: *B. aereus*; Sil: silybin.

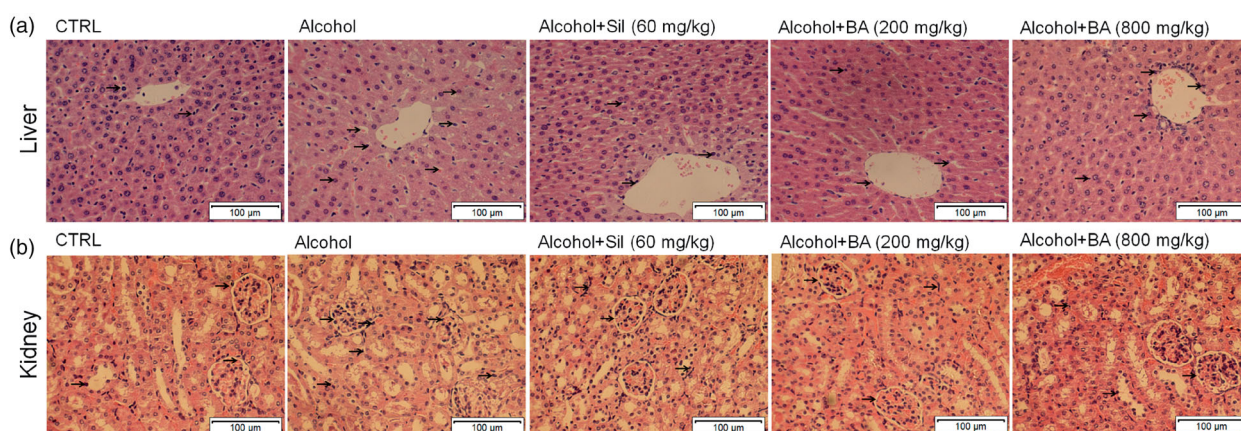


Figure 2. The protection of BA against alcohol caused liver damage. Histopathological analysis in (a) liver and (b) kidney detecting by H&E staining (Scale bar: 100 μ m; magnification: 400 \times). The arrows indicate pathological changes (Inflammatory cells, shrivelled nuclei and swollen of hepatic cells or fat vacuoles diffuse in liver; inflammatory cells, glomerular hyperaemia or tubular epithelial cell edema in kidney). BA: *B. aereus*; Sil: silybin.

AST and ALT serve as biomarkers for liver function, directly reflecting the degree of liver injury. ADH and ALDH are the main enzymes responsible for alcohol metabolism (Kaviarasan and Anuradha 2007). Compared with the healthy mice, extremely high levels of AST (>15.6%) and ALT (>12.9%), and low levels of ADH (23.1%) and ALDH (>14.0%) in the liver and/or serum, were noted in the alcohol-only treated mice ($p < 0.05$; Table 2). Compared with the alcohol-only treated mice, similar to Sil, BA only strongly enhanced the levels of ALDH (>18.9%) in the serum ($p < 0.05$; Table 2). In the liver, BA treatment remarkably reduced the levels of AST (>27.6%) and ALT (>18.3%) ($p < 0.05$; Table 2), and enhanced the levels of ADH (>35.0%) ($p < 0.01$; Table 2). Sil regulated the levels of AST, ADH and ALDH ($p < 0.05$; Table 2), but not ALT ($p > 0.05$; Table 2).

Heavy drinking can attenuate the oxidation of fatty acids and the deposition of fat in the blood and liver cells, resulting in the accumulation of TC and a substantial reduction in HDL (Tang et al. 2017). Compared with the non-alcohol-treated healthy mice, elevated TC levels and suppressed HDL levels were observed in the liver of the alcohol-only treated mice ($p < 0.05$; Figure 1), which were regulated back to their normal levels by BA ($p < 0.01$; Figure 1). BA at 800 mg/kg failed to enhance the

hepatic levels of HDL (Figure 1(b)). Sil only enhanced the low hepatic level of HDL in the alcohol-damaged mice ($p < 0.001$; Figure 1(b)).

Pathological section image analysis revealed that the hepatic lobule structure was damaged in the alcohol-only treated mice, manifested by the disordered arrangement of hepatic cells, shrivelled nuclei, swollen hepatocytes, diffuse fat vacuoles and infiltration of inflammatory cells (Figure 2(a)), which were all alleviated by BA administration (Figure 2(a)).

Glomerular hyperaemia, tubular epithelial cell edema, narrow stenosis and interstitial infiltration of inflammatory cells were noted in the kidneys of the alcohol-only treated mice (Figure 2(b)). Comparatively, the alcohol-induced renal injury was significantly reduced in the BA-treated mice, and only mild edema and inflammatory cell infiltration were observed (Figure 2(b)).

Effects of BA on inflammatory cytokines

Alcohol causes the accumulation of inflammatory factors in the liver of mice, leading to the occurrence of hepatitis (Fung and

Table 3. The Effects of BA and Sil on anti-inflammatory activity of serum, liver in alcohol-treated mice.

	Alcohol (13 g/kg)				
	CTRL	Model	Sil (60 mg/kg)	BA (200 mg/kg)	BA (800 mg/kg)
Serum					
CXCL13 (pg/mL)	499.8 ± 6.3	564.8 ± 10.1 [#]	504.5 ± 9.0*	599.5 ± 44.7	480.4 ± 17.8*
YKL-40 (ng/mL)	52.8 ± 1.3	62.1 ± 2.8 [#]	52.9 ± 2.3*	64.6 ± 4.0	53.8 ± 1.7*
TPO (pg/mL)	97.2 ± 2.3	86.0 ± 1.5 [#]	96.0 ± 3.1*	101.4 ± 2.7*	97.4 ± 4.2*
IL-7 (pg/mL)	87.5 ± 2.1	102.5 ± 2.8 [#]	95.2 ± 3.0	109.4 ± 2.4	93.7 ± 1.2
PAI-1 (pg/mL)	924.8 ± 14.5	980.7 ± 13.9	915.0 ± 25.7	731.3 ± 6.6**	837.6 ± 12.7*
RBP4 (µg/mL)	38.0 ± 0.3	33.7 ± 0.4 [#]	36.8 ± 0.8	36.1 ± 0.3	34.3 ± 1.2
Liver					
CXCL13 (pg/mg)	184.7 ± 3.5	217.6 ± 5.6 [#]	188.0 ± 5.0*	181.3 ± 8.0*	205.3 ± 11.3
YKL-40 (ng/mg)	22.3 ± 0.4	28.7 ± 0.5 ^{##}	23.2 ± 0.7*	21.7 ± 1.0**	22.2 ± 1.1**
TPO (pg/mg)	50.0 ± 1.1	40.9 ± 1.4 [#]	51.5 ± 1.3**	43.3 ± 1.5	44.9 ± 2.7
IL-7 (pg/mg)	35.7 ± 0.8	43.2 ± 1.4 ^{##}	34.6 ± 1.2*	37.7 ± 0.7*	45.2 ± 1.4
PAI-1 (pg/mg)	287.8 ± 6.5	341.3 ± 10.8 [#]	294.8 ± 7.9*	263.2 ± 8.4**	292.2 ± 19.3*
RBP4 (µg/mg)	14.2 ± 0.3	11.1 ± 0.2 ^{##}	15.1 ± 0.3**	12.5 ± 0.4*	13.8 ± 0.4**

All data are presented as mean ± S.E.M. (n = 10).

[#]p < 0.05, ^{##}p < 0.01 compared with control group; *p < 0.05 and **p < 0.01 compared with alcohol group.

Table 4. The effects of BA and Sil on antioxidant status of serum and liver in alcohol-treated mice.

	Alcohol (13 g/kg)				
	CTRL	Model	Sil (60 mg/kg)	BA (200 mg/kg)	BA (800 mg/kg)
Serum					
ROS (U/mL)	342.2 ± 5.7	356.7 ± 3.6	329.0 ± 3.2	349.8 ± 15.1	338.6 ± 3.3
MDA (nmol/mL)	18.4 ± 0.3	20.6 ± 0.5 [#]	18.8 ± 0.4	17.5 ± 0.4*	18.4 ± 0.7*
NO (µmol/L)	28.7 ± 0.8	33.7 ± 1.1 [#]	30.5 ± 1.2	35.0 ± 1.6	32.4 ± 1.9
SOD (U/mL)	214.7 ± 7.4	161.8 ± 4.3 ^{##}	199.2 ± 4.2**	196.1 ± 5.4**	183.5 ± 6.3*
GSH-Px (U/mL)	269.1 ± 5.9	233.6 ± 2.8 [#]	261.4 ± 6.0*	287.8 ± 7.1**	259.4 ± 6.0*
CAT (U/mL)	43.6 ± 0.8	37.2 ± 1.0 [#]	44.2 ± 0.5*	46.1 ± 1.1**	39.0 ± 0.7
Liver					
ROS (U/mg)	161.2 ± 2.6	205.4 ± 6.2 ^{##}	184.3 ± 3.2*	151.4 ± 10.8**	157.6 ± 9.4**
MDA (nmol/mg)	4.9 ± 0.1	5.7 ± 0.2 [#]	5.4 ± 0.1	4.7 ± 0.4*	4.5 ± 0.4**
NO (µmol/g)	14.2 ± 0.2	16.1 ± 0.8 [#]	14.5 ± 0.3	17.1 ± 0.7	10.5 ± 0.7**
SOD (U/mg)	91.6 ± 2.1	70.1 ± 2.4 ^{##}	112.5 ± 3.7***	103.6 ± 6.4**	81.6 ± 7.6*
GSH-Px (U/mg)	101.6 ± 1.4	83.4 ± 2.1 [#]	114.8 ± 2.6**	120.7 ± 1.1**	98.8 ± 7.0*
CAT (U/mg)	25.0 ± 0.4	19.7 ± 0.5 ^{##}	24.9 ± 0.6**	22.3 ± 0.7*	20.1 ± 1.2

The antioxidant status was measured in mice serum and liver. All data are presented as mean ± S.E.M. (n = 10).

[#]p < 0.05, ^{##}p < 0.01 compared with control group; *p < 0.05, **p < 0.01 and ***p < 0.001 compared with alcohol group.

Pyrsoopoulos 2017). Here, acute alcohol exposure-induced dramatic increases in the levels of CXCL13 (17.8%), YKL-40 (28.7%), IL-7 (21.0%) and PAI-1 (18.6%), and reductions in the levels of TPO (18.2%) and RBP4 (21.8%) in the liver. These changes were strongly suppressed by BA administration, except for the TPO ($p < 0.05$; Table 3). Enhanced levels of CXCL13 (13.0%), YKL-40 (17.6%) and IL-7 (17.1%), and reduced levels of TPO (11.5%) and RBP4 (11.3%) in the serum, were noted in the acute alcohol-exposed mice, compared with the healthy mice ($p < 0.05$; Table 3). Comparatively, BA administration resulted in the reduction of serum levels of CXCL13 (14.9% in dose of 800 mg/kg), YKL-40 (13.4% in dose of 800 mg/kg), PAI-1 (>14.6%) and the enhancement of serum level of TPO (>13.3%) ($p < 0.05$; Table 3). The non-dose-dependent manner of BA was noted during its regulation on the levels of inflammatory cytokines. Furthermore, BA failed to influence the serum levels of IL-7 and RBP4 in the acute alcohol-exposed mice (Table 3). Sil administration significantly regulated the levels of all six chosen factors in the liver, but showed beneficial effects only on CXCL13, YKL-40 and TPO in the serum of the acute alcohol-exposed mice ($p < 0.05$; Table 3).

Antioxidative effect of BA

Excessive ROS and MDA can induce lipid peroxidation and trigger degradation processes, thus affecting the cell membrane

(Wen et al. 2017). NO can induce the production of cytokines and mediate the inflammatory response in the late stage of oxidative stress (Zhao et al. 2017). Extremely high levels of ROS (27.4%), MDA (16.3%), NO (13.4%) and low activities of SOD (23.5%), GSH-Px (17.9%) and CAT (21.2%) were noted in the liver of the mice with alcohol-induced hepatotoxicity compared with healthy mice ($p < 0.05$; Table 4), which were all restored to healthy levels by 14-day BA administration ($p < 0.05$; Table 4). In the acute alcohol-exposed mice, similar changes of oxidative factors were noted in the serum as in the liver samples ($p < 0.05$; Table 4), except for the ROS levels, which were not changed significantly. The 14-day administration of BA strongly reduced the hyper-level of MDA (>10.7%), and enhanced the hypo-levels of SOD (>13.4%), GSH-Px (>11.0%), CAT (23.9% in dose of 200 mg/kg) in the serum of the mice with alcohol-induced hepatotoxicity ($p < 0.05$; Table 4). Sil significantly regulated the chosen oxidative factors in both serum and liver ($p < 0.05$; Table 4), except for ROS, MDA and NO in the serum, and MDA and NO in the liver (Table 4).

Effects of BA on the activation of NF-κB p65

In the process of alcohol metabolism, ROS can activate the NF-κB signalling, which is responsible for accelerating the synthesis of inflammatory mediators (Zhou et al. 2018). Compared with

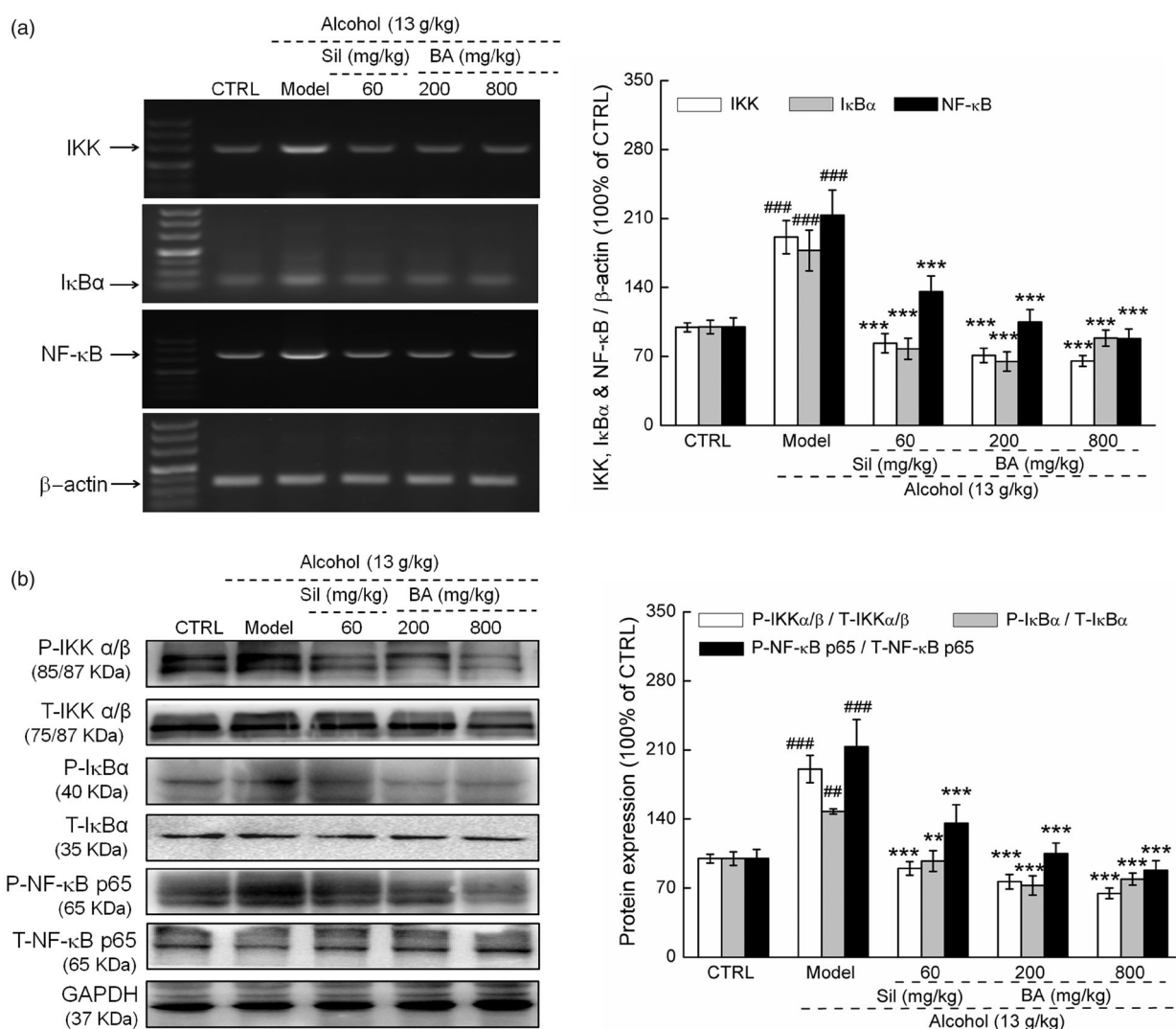


Figure 3. NF- κ B signalling is involved in the protection of BA against acute alcohol-induced liver damage in the C57BL/6 mouse. (a) The mRNA expression of IKK, I κ B α and NF- κ B were measured by RT-PCR in the liver of mice with acute alcohol-induced liver injury. BA and Sil significantly suppressed their expressions after 2-week treatment. Marker size from top to bottom: 500, 400, 300, 200, 150, 100 and 50 bp. The data on quantified mRNA expression were normalized to the levels of β -actin ($n = 6$). (b) Two-week BA and Sil treatment suppressed the levels of phosphor-IKK α/β , phosphor-I κ B α and phosphor-NF- κ B p65 in the livers of mice with acute alcohol-induced liver injury. The data on quantified protein expression were normalized to the levels of GAPDH ($n = 10$). The data were analyzed using a one-way ANOVA and they are expressed as means \pm S.E.M. ### $p < 0.01$ and ### $p < 0.001$ vs. non-alcohol control group; ** $p < 0.01$ and *** $p < 0.001$ vs. alcohol-treated model group. BA: *B. aereus*; Sil: silybin.

healthy mice, acute alcohol administration caused the enhancement of the mRNA levels of IKK, I κ B α and NF- κ B (>70.0%) in liver, which were strongly suppressed by BA and Sil ($p < 0.001$; Figure 3(a)). Furthermore, the enhanced phosphorylated expressions of IKK α/β , I κ B α , and NF- κ B p65 (>45.0%) in the liver of the mice induced by acute alcohol exposure were all successfully suppressed after 14-day BA and Sil administration ($p < 0.01$; Figure 3(b)).

Discussion

In this study, we confirmed the hepatoprotective effect of BA in mice with acute alcohol-induced hepatotoxicity, and clarified the mechanisms related to oxidative stress-mediated NF- κ B signalling. BA, an edible fungus, contains 21 fatty acids, 17 amino acids and 13 minerals, indicating its extremely high nutritive value. The detection of zero or low levels of heavy metals suggests that BA is safe for consumption. Potential antioxidants such as vitamins, total polyphenols, and total sterols were

detected in BA, which regulate oxidative stress in the body and reduce ROS production, thereby inhibiting the activation of the NF- κ B signalling pathway. The total flavonoids in *Polygoni Perfoliati Herba* previously showed anti-lipid peroxidation and anti-inflammation effects in mice with alcohol-induced liver injury (Ya et al. 2016). A triterpene from the bark of *Betula platyphylla* Suk. (Betulaceae) alleviates alcoholic liver injury, possibly through blocking fatty acid synthesis and activating the adenosine monophosphate-activated protein kinase (AMPK) signalling pathway (Bai et al. 2016). BA is rich in polysaccharides, total flavonoids, vitamins, polyphenols and triterpenoids, which provide a strong nutritional foundation for its hepatoprotective effect. Additionally, the detection of multiple active compounds in BA allows us to explain the non-dose-dependence manner during its hepatic protection, which is in fact a common feature of pharmaceutically active natural products (Ma et al. 2015).

Alcohol is first metabolized to acetaldehyde by ADH, after which acetaldehyde is metabolized to acetic acid by ALDH (Jelski et al. 2008). Heavy drinking results in a decrease of the

activities of the ADH and ALDH enzymes, which eventually leads to over-accumulation of acetaldehyde in the liver. This triggers the immune system, resulting in inflammation and severe liver damage, highlighted by large increases in the levels of AST and ALT activity, pro-oxidation enzymes and inflammatory cytokines (Karpyak et al. 2017). Our data confirmed the protective effects of BA against acute alcohol hepatotoxicity. A large number of adipocytes were noted in the liver of the mice with acute alcohol exposure. As the synthesis and degradation of cholesterol are mainly carried out in the liver, TC levels directly reflect the liver's reserve function (Komorovskiy 1998). HDL is also mainly synthesized by the liver, and is considered as an important indicator of coronary artery disease in clinics (Ayhan et al. 2017). BA significantly enhanced the HDL levels and reduced the TC content in the liver, indicating its regulation of the abnormal alternations of lipid metabolism caused by acute alcohol exposure.

It has been confirmed that BA has the regulation effect on oxidative stress (Zhang et al. 2018), which is recognized as a crucial causal factor of acute alcohol-induced liver injury. This is especially the case when the liver has lower levels of antioxidant protection to cope with the generation of ROS (Diaz-Aguirre et al. 2016). ROS and MDA cause oxidative damage to biological macromolecules including nucleic acids and proteins (Sun et al. 2018). As another important factor of oxidative stress, NO is responsible for the formation of hydroxyl radicals, which contribute to alcohol-induced liver damage (Yamasaki et al. 2001). Encouragingly, BA not only reduced the hyper-levels of oxidative factors, but also increased the activities of antioxidative factors in the serum and liver of mice with acute alcohol injury. The nicotinamide adenine dinucleotide phosphate (NADPH) oxidase complex converts O_2 to superoxide ($O_2^{\bullet-}$) to produce ROS. In contrast, SOD converts superoxide into H_2O_2 and CAT converts H_2O_2 into H_2O (Nordberg and Arnér 2001). Previous research suggests that the hepatoprotective effects on alcohol-induced liver oxidative injury are due to antioxidant enzymes (Li et al. 2015). All of the above studies support our conclusion that the antioxidative properties of BA played a central role during its hepatoprotective effect on mice with alcohol-induced liver damage.

Alcohol ingestion activates the innate immune system by regulating the secretion of inflammatory cytokines (Zhao et al. 2015). The over-accumulation of NO caused by alcohol exposure induces the production of cytokines mediating the late inflammatory response of oxidative stress (Adua et al. 2015). YKL40 is highly expressed in chronic liver disease patients with liver fibrosis and cirrhosis (Sarma et al. 2012). As reported, the link between YKL-40 and ALD is mediated by ROS (Gerin et al. 2016). PAI-1 inhibits fibrin degradation, promotes fibrin deposition on blood vessel walls, and stimulates smooth muscle cell proliferation (Hasenstab et al. 2000). ROS can promote the release of PAI-1, the synthesis of PAI-1 mRNA, and the activation of the PAI-1 gene promoter (Swiatkowska et al. 2002). BA displayed hepatoprotection against alcohol-induced liver damage via its modulation of inflammatory cytokines, which may be also associated with oxidative stress.

BA strongly inhibited the phosphorylation of NF- κ B p65 by inhibiting the phosphorylation of IKK α / β and I κ B α . Exogenous stimuli can activate the NF- κ B signalling pathway, leading to activation of I κ B kinase. This results in the phosphorylation of I κ B protein, causing the degradation of I κ B protein, and then releasing NF- κ B (Wu et al. 2014). Upon activation via post-translational modifications, NF- κ B is transferred to the nucleus,

where it promotes the transcription of the target genes. Nuclear NF- κ B mediates transcription of the IL-7 receptor α -subunit (CD127) (Miller et al. 2014) and YKL-40 (Bhat et al. 2008). Meanwhile, NF- κ B can activate the transcription of the CXCL13 gene (Garg et al. 2017) and regulate the expression of PAI-1 and RBP4 (Swiatkowska et al. 2002; Zhou et al. 2016). Conversely, ROS can be produced by the degradation of I κ B, resulting in the phosphorylation of p65 (Shi et al. 2018), thereby inducing binding of NF- κ B to target sequences in the nucleus encoding the production of inflammatory factors (Lingappan 2018). Alcohol-induced oxidative stress can lead to an increase in the levels of pro-inflammatory cytokines, such as TNF- α or IL-1 β (Galicia-Moreno and Gutiérrez-Reyes 2014). In this article, we have successfully confirmed that BA protects against acute alcohol-induced liver damage in mice via modulation of the oxidative stress-related NF- κ B signalling, which is similar to our research on how *Antrodia cinnamomea* protects against acute alcohol-induced liver damage in mice (Liu et al. 2017).

The present study has limitations. Acute alcohol-induced liver injury can be caused after just 2 weeks; however, the level of hepatocyte swelling and the number of fat vacuoles are less than those in mice affected by chronic alcohol consumption (Song et al. 2016). In patients with chronic alcohol drinking, ALT/AST and hepatic steatosis can be significantly increased, leading to increased risk of death (Marin et al. 2017). Therefore, further research will be performed in mice with chronic alcohol-induced liver damage to investigate the protection of BA. Furthermore, based on the results obtained from this study, it is hard for us to conclude which component contained in BA shows the specific liver protection. Our ongoing experiments have found that the polysaccharides contained in BA may be one of the specific components to show the protection of liver injury. However, more experiments need to be performed to confirm the roles of BA polysaccharides.

The novelty of this study is the first systematic analysis of the nutrient composition of BA, confirmation of its hepatoprotective effect on alcohol-induced acute liver injury in mice, and evidence of its possible protective mechanisms related to the regulation of the oxidative stress-mediated NF- κ B signalling.

Disclosure statement

The authors have declared that there is no conflict of interest.

Funding

This work was supported by the Science and Technology Development Project in Jilin Province of China under grant [No. 20191102027YY, 20200708091YY and 20200708068YY], the Special Projects of Cooperation between Jilin University and Jilin Province in China under grant [No. SXGJSF2017-1], Innovation Training Program of Zhuhai College of Jilin University under grant [No. 2018XJCQ016], and "Three levels" Talent Construction Projects in Zhuhai College of Jilin University.

References

- Abhilash PA, Harikrishnan R, Indira M. 2014. Ascorbic acid suppresses endotoxemia and NF- κ B signaling cascade in alcoholic liver fibrosis in guinea pigs: a mechanistic approach. *Toxicol Appl Pharmacol.* 274(2): 215–224.

- Adua E, Danso FO, Boa-Amponsem OM, Adusei-Mensah F. 2015. Effect of neutrophils on nitric oxide production from stimulated macrophages. *Iran J Immunol.* 12:94–103.
- Araújo LBDC, Silva SL, Galvão MAM, Ferreira MRA, Araújo EL, Randau KP, Soares LAL. 2013. Total phytosterol content in drug materials and extracts from roots of *Acanthospermum hispidum* by UV-vis spectrophotometry. *Rev Bras Farmacogn.* 23(5):736–742.
- Ayhan H, Gormus U, Isbir S, Yilmaz SG, Isbir T. 2017. SCARB1 gene polymorphisms and HDL subfractions in coronary artery disease. *In Vivo.* 31(5):873–876.
- Bai T, Yang Y, Yao YL, Sun P, Lian LH, Wu YL, Nan JX. 2016. Betulin alleviated ethanol-induced alcoholic liver injury via sirt1/ampk signaling pathway. *Pharmacol Res.* 105:1–12.
- Beugelsdijk DC, van der Linde S, Zuccarello GC, den Bakker HC, Draisma SG, Noordeloos ME. 2008. A phylogenetic study of *Boletus* section *Boletus* in Europe. *Persoonia.* 20:1–7.
- Bhat KP, Pelloski CE, Zhang Y, Kim SH, deLaCruz C, Rehli M, Aldape KD. 2008. Selective repression of YKL-40 by NF-kappaB in glioma cell lines involves recruitment of histone deacetylase-1 and -2. *FEBS Lett.* 582(21–22):3193–3200.
- Bubici C, Papa S, Dean K, Franzoso G. 2006. Mutual cross-talk between reactive oxygen species and nuclear factor-kappa B: molecular basis and biological significance. *Oncogene.* 25(51):6731–6748.
- Chromy V, Vinklarkova B, Sprongl L, Bittova M. 2015. The Kjeldahl method as a primary reference procedure for total protein in certified reference materials used in clinical chemistry. I. A review of Kjeldahl methods adopted by laboratory medicine. *Crit Rev Anal Chem.* 45:106–111.
- Dai C, Li D, Gong L, Xiao X, Tang S. 2016. Curcumin ameliorates furazolidone-induced DNA damage and apoptosis in human hepatocyte l02 cells by inhibiting ROS production and mitochondrial pathway. *Molecules.* 21(8):1061–1015.
- Diaz-Aguirre V, Velez-Pardo C, Jimenez-Del-Rio M. 2016. Fructose sensitizes Jurkat cells oxidative stress-induced apoptosis via caspase-dependent and caspase-independent mechanisms. *Cell Biol Int.* 40(11):1162–1173.
- Farfan Labonne BE, Gutierrez M, Gomez-Quiroz LE, Konigsberg Fainstein M, Bucio L, Souza V, Flores O, Ortiz V, Hernandez E, Kershenovich D, et al. 2009. Acetaldehyde-induced mitochondrial dysfunction sensitizes hepatocytes to oxidative damage. *Cell Biol Toxicol.* 25(6):599–609.
- Fung P, Pysopoulos N. 2017. Emerging concepts in alcoholic hepatitis. *World J Hepatol.* 9(12):567–585.
- Galicia-Moreno M, Gutiérrez-Reyes G. 2014. The role of oxidative stress in the development of alcoholic liver disease. *Rev Gastroenterol Mex.* 79(2): 135–144.
- Gao B, Bataller R. 2011. Alcoholic liver disease: pathogenesis and new therapeutic targets. *Gastroenterology.* 141(5):1572–1585.
- Garg R, Blando JM, Perez CJ, Abba MC, Benavides F, Kazanietz MG. 2017. Protein kinase c epsilon cooperates with pten loss for prostate tumorigenesis through the CXCL13-CXCR5 pathway. *Cell Rep.* 19(2):375–388.
- Gerin F, Erman H, Erbogha M, Sener U, Yilmaz A, Seyhan H, Gurel A. 2016. The effects of ferulic acid against oxidative stress and inflammation in formaldehyde-induced hepatotoxicity. *Inflammation.* 39(4):1377–1386.
- Guo YY, Jie XU, Xing J, Wang MJ, Tao MX. 2015. Improvement effect of polysaccharides from *Boletus aereus* on alcoholic liver injury in mice serum. *Sci Tech Food Ind.* 36(24):325–328.
- Hasenstab D, Lea H, Clowes AW. 2000. Local plasminogen activator inhibitor type 1 overexpression in rat carotid artery enhances thrombosis and endothelial regeneration while inhibiting intimal thickening. *Arterioscler Thromb Vasc Biol.* 20(3):853–859.
- Hurel C, Tanez M, Volpi Ghirardini A, Libralato G. 2017. Effects of mineral amendments on trace elements leaching from pre-treated marine sediment after simulated rainfall events. *Environ Pollut.* 220(Pt A):364–374.
- Jain VM, Karibasappa GN, Dodamani AS, Mali GV. 2017. Estimating the carbohydrate content of various forms of tobacco by phenol-sulfuric acid method. *J Educ Health Promot.* 6:1–6.
- Jelski W, Zalewski B, Szmítkowski M. 2008. Alcohol dehydrogenase (ADH) isoenzymes and aldehyde dehydrogenase (ALDH) activity in the sera of patients with liver cancer. *J Clin Lab Anal.* 22(3):204–209.
- Karpyak V, Biernacka J, Geske J, Batzler A, Hall-Flavin D, Loukianova L, Schneekloth T, Skime M, Frye M, Choi D-S. 2017. M64 - genome-wide association analyses reveal SNP-by-consumption interaction effects on ALT and AST levels in alcohol dependent patients. *Eur Neuropsychopharmacol.* 27:S412.
- Kaviarasan S, Anuradha CV. 2007. Fenugreek (*Trigonella foenum graecum*) seed polyphenols protect liver from alcohol toxicity: a role on hepatic detoxification system and apoptosis. *Pharmazie.* 62(4):299–304.
- Komorov'skyi RR. 1998. Liver function and the level of total cholesterol in the blood serum in liver cirrhosis. *Lik Sprava.* (8):83–85. <https://pubmed.ncbi.nlm.nih.gov/10204356/>.
- Kosani M, Rankovi B, Ran A, I i, Stanojkovi T. 2017. Evaluation of metal contents and bioactivity of two edible mushrooms *Agaricus campestris* and *Boletus edulis*. *Emir J Food Agric.* 29(2):98–103.
- Krpan M, Vahčić N, Hruškar M. 2009. Validation of an HPLC method for the determination of nucleotides in infant formulae. *J Liq Chromatogr Relat Technol.* 32(18):2747–2755.
- Lemieszek MK, Ribeiro M, Marques G, Nunes FM, Pożarowski P, Rzeski W. 2017. New insights into the molecular mechanism of *Boletus edulis* ribonucleic acid fraction (BE3) concerning antiproliferative activity on human colon cancer cells. *Food Funct.* 8(5):1830–1839.
- Li JJ, Hu XQ, Zhang XF, Liu JJ, Cao LS. 2014. Study on variation of main ingredients from spores and fruiting bodies of *Ganoderma lucidum*. *Zhongguo Zhong Yao Za Zhi.* 39:4246–4251.
- Li W, Qu XN, Han Y, Zheng SW, Wang J, Wang YP. 2015. Ameliorative effects of 5-hydroxymethyl-2-furfural (5-HMF) from *Schisandra chinensis* on alcoholic liver oxidative injury in mice. *IJMS.* 16(2):2446–2457.
- Lingappan K. 2018. NF-κB in oxidative stress. *Curr Opin Toxicol.* 7:81–86.
- Liu Y, Wang J, Li L, Hu W, Qu Y, Ding Y, Meng L, Teng L, Wang D. 2017. Hepatoprotective effects of *Antrodia cinnamomea*: the modulation of oxidative stress signaling in a mouse model of alcohol-induced acute liver injury. *Oxid Med Cell Longev.* 2017:1–12.
- Ma L, Zhang S, Du M. 2015. Cordycepin from *Cordyceps militaris* prevents hyperglycemia in alloxan-induced diabetic mice. *Nutr Res.* 35(5):431–439.
- Manurung H, Kustiawan W, Kusuma IW, Marjenah M. 2017. Total flavonoid content and antioxidant activity in leaves and stems extract of cultivated and wild tabat barito (*Ficus deltoidea* Jack). *AIP Conf Proc.* 1813(1): 020007-1-6.
- Marin V, Poulsen K, Odena G, McMullen MR, Altamirano J, Sancho-Bru P, Tiribelli C, Caballeria J, Rosso N, Bataller R, et al. 2017. Hepatocyte-derived macrophage migration inhibitory factor mediates alcohol-induced liver injury in mice and patients. *J Hepatol.* 67(5):1018–1025.
- Mattila P, Konko K, Euroala M, Pihlava JM, Astola J, Vahteristo L, Hietaniemi V, Kumpulainen J, Valtonen M, Piironen V. 2001. Contents of vitamins, mineral elements, and some phenolic compounds in cultivated mushrooms. *J Agric Food Chem.* 49(5):2343–2348.
- Miller ML, Mashayekhi M, Chen L, Zhou P, Liu X, Michelotti M, Tramontini Gunn N, Powers S, Zhu X, Evaristo C, et al. 2014. Basal NF-κB controls IL-7 responsiveness of quiescent naïve T cells. *Proc Natl Acad Sci USA.* 111(20):7397–7402.
- Musci M, Yao S. 2017. Optimization and validation of Folin-Ciocalteu method for the determination of total polyphenol content of Pu-erh tea. *Int J Food Sci Nutr.* 68(8):913–918.
- Nordberg J, Arnér ESJ. 2001. Reactive oxygen species, antioxidants, and the mammalian thioredoxin system. *Free Radic Biol Med.* 31:1287–1312.
- Ozkol H, Bulut G, Balahoroglu R, Tuluce Y, Ozkol HU. 2017. Protective effects of selenium, N-acetylcysteine and vitamin E against acute ethanol intoxication in rats. *Biol Trace Elem Res.* 175(1):177–185.
- Ren Y, Geng Y, Chen H, Lu Z-M, Shi J-S, Xu Z. 2018. Polysaccharide peptides from *Coriolus versicolor*: a multi-targeted approach for the protection or prevention of alcoholic liver disease. *J Funct Foods.* 40:769–777.
- Rivera-Jacinto M, Rodríguez-Ulloa C, Huayán-Dávila G. 2009. Frecuencia de aislamientos ambientales de *Staphylococcus aureus* y su actividad beta-lactamasa en un hospital de Cajamarca, Perú. *Infectio.* 13(3):192–195.
- Sarma NJ, Tiriveedhi V, Subramanian V, Shenoy S, Crippin J, Chapman W, Mohanakumar T. 2012. 17-OR: Modulation of microRNA-449a by hepatitis c virus (HCV) in regulating expression of the inflammatory biomarker YKL40 through targeting components of the notch/NF kappa B signaling pathways. *Hum Immunol.* 73:14–14.
- Setshedi M, Wands JR, Monte SM. 2010. Acetaldehyde adducts in alcoholic liver disease. *Oxid Med Cell Longev.* 3(3):178–185.
- Shi X-m, Xu G-m, Zhang G-j, Liu J-r, Wu Y-m, Gao L-g, Yang Y, Chang Z-s, Yao C-w. 2018. Low-temperature plasma promotes fibroblast proliferation in wound healing by ROS-activated NF-κB signaling pathway. *Curr Med Sci.* 38(1):107–114.
- Smith CR, Tschinkel WR. 2009. Ant fat extraction with a Soxhlet extractor. *Cold Spring Harb Protoc.* 2009(7):5243.
- Song M, Chen T, Prough RA, Cave MC, McClain CJ. 2016. Chronic alcohol consumption causes liver injury in high-fructose-fed male mice through enhanced hepatic inflammatory response. *Alcohol Clin Exp Res.* 40(3): 518–528.
- Sun J, Lin H, Zhang S, Lin Y, Wang H, Lin M, Hung Y-C, Chen Y. 2018. The roles of ROS production-scavenging system in *Lasiodiplodia theobromae* (Pat.) Griff. & Maubl.-induced pericarp browning and disease development of harvested longan fruit. *Food Chem.* 247:16–22.

- Swiatkowska M, Szemraj J, Al-Nedawi KNI, Pawłowska Z. 2002. Reactive oxygen species upregulate expression of PAI-1 in endothelial cells. *Cell Mol Biol Lett.* 7(4):1065–1071.
- Tang X, Wei R, Deng A, Lei T. 2017. Protective effects of ethanolic extracts from artichoke, an edible herbal medicine, against acute alcohol-induced liver injury in mice. *Nutrients.* 9(9):1000–1012.
- Triantafyllou K, Vlachogiannakos J, Ladas SD. 2010. Gastrointestinal and liver side effects of drugs in elderly patients. *Best Pract Res Clin Gastroenterol.* 24(2):203–215.
- Wen J, Wu Y, Wei W, Li Z, Wang P, Zhu S, Dong W. 2017. Protective effects of recombinant human cytoglobin against chronic alcohol-induced liver disease *in vivo* and *in vitro*. *Sci Rep.* 7:41647.
- Wu S, Wang G, Yang R, Cui Y. 2016. Anti-inflammatory effects of *Boletus edulis* polysaccharide on asthma pathology. *Am J Transl Res.* 8: 4478–4489.
- Wu J, Xue X, Wu Z, Zhao H-L, Cao H-M, Sun D-Q, Wang R-M, Sun J, Liu Y, Guo R-C. 2014. Anti-tumor effect of paeonol via regulating NF- κ B, AKT and MAPKs activation: a quick review. *Biomed Prevent Nut.* 4(1): 9–14.
- Ya GAO, Houkang CAO, Simao H, Kefeng Z. 2016. Protective effect and acting mechanism of total flavonoids of *Polygoni perfoliati* herba on acute alcohol-induced liver injury in mice. *Med Plant.* 7(3/4):21–32.
- Yamasaki H, Shimoji H, Ohshiro Y, Sakihama Y. 2001. Inhibitory effects of nitric oxide on oxidative phosphorylation in plant mitochondria. *Nitric Oxide.* 5(3):261–270.
- Zhang X, Chen Y, Cai G, Li X, Wang D. 2017. Carnosic acid induces apoptosis of hepatocellular carcinoma cells via ROS-mediated mitochondrial pathway. *Chem Biol Interact.* 277:91–100.
- Zhang L, Hu Y, Duan X, Tang T, Shen Y, Hu B, Liu A, Chen H, Li C, Liu Y. 2018. Characterization and antioxidant activities of polysaccharides from thirteen *Boletus* mushrooms. *Int J Biol Macromol.* 113:1–7.
- Zhang N, Li Q, Wang J, Lu J, Yang S, Xie J, Meng Q, Quan Y, Wang D, Teng L. 2014. Screening of *Irpex lacteus* mutant strains and optimizing fermentation conditions. *J Food Agric Environ.* 12:1213–1219.
- Zhao Z, Gong S, Wang S, Ma C. 2015. Effect and mechanism of evodiamine against ethanol-induced gastric ulcer in mice by suppressing Rho/NF- κ B pathway. *Int Immunopharmacol.* 28(1):588–595.
- Zhao X, Wang L, Zhang H, Zhang D, Zhang Z, Zhang J. 2017. Protective effect of artemisinin on chronic alcohol induced-liver damage in mice. *Environ Toxicol Pharmacol.* 52:221–226.
- Zheng J-Q, Wang J-Z, Shi C-W, Mao D-B, He P-X, Xu C-P. 2014. Characterization and antioxidant activity for exopolysaccharide from submerged culture of *Boletus aereus*. *Process Biochem.* 49(6): 1047–1053.
- Zhou W, Ye S, Li J. 2016. Expression of retinol binding protein 4 and nuclear factor- κ B in diabetic rats with atherosclerosis and the intervention effect of pioglitazone. *Exp Ther Med.* 12(2):1000–1006.
- Zhou J, Zhang J, Wang C, Qu S, Zhu Y, Yang Z, Wang L. 2018. Açai (*Euterpe oleracea* Mart.) attenuates alcohol-induced liver injury in rats by alleviating oxidative stress and inflammatory response. *Exp Ther Med.* 15(1):166–172.